


Article

A Step Forward to the Characterization of Secondary Effluents to Predict Membrane Fouling in a Subsequent Ultrafiltration

Anderson Alejandro Benites-Zelaya, José Luis Soler-Cabezas , Eva Ferrer-Polonio, José Antonio Mendoza-Roca * and María Cinta Vincent-Vela 

Instituto de Seguridad Industrial, Radiofísica y Medioambiental, Universitat Politècnica de València, Camino de Vera, s/n, 46022 Valencia, Spain; anbeze@posgrado.upv.es (A.A.B.-Z.); jsoca@isiryum.upv.es (J.L.S.-C.); evferpo@posgrado.upv.es (E.F.-P.); mavinve@iqn.upv.es (M.C.V.-V.)

* Correspondence: jamendoz@iqn.upv.es

Received: 13 June 2020; Accepted: 7 July 2020; Published: 13 July 2020



Abstract: Nowadays, wastewater reuse in Mediterranean countries is necessary to cover the water demand. This contributes to the protection of the environment and encourages the circular economy. Due to increasingly strict regulation, the secondary effluent of a wastewater treatment plant requires further (tertiary) treatment to reach enough quality for its reuse in agriculture. Ultrafiltration is a membrane technique suitable for tertiary treatment. However, the most important drawback of ultrafiltration is membrane fouling. The aim of this work is to predict membrane fouling and ultrafiltered wastewater permeate quality for a particular membrane, using the information given by an exhaustive secondary effluent characterization. For this, ultrafiltration of real and simulated wastewaters and of their components after fractionation has been performed. In order to better characterize the secondary effluent, resin fractionation and further membrane ultrafiltration of the generated fractions and wastewater were performed. The results indicated that hydrophobic substances were lower than hydrophilic ones in the secondary effluent. Supelite DAX-8, Amberlite XAD-4 and Amberlite IRA-958 resins were found not to be specific for humic acids, proteins and carbohydrates, which are the main components of the effluent organic matter. Two models have been performed using statistics (partial least squares, PLS) and an artificial neural network (ANN), respectively. The results showed that the ANN model predicted permeate quality and membrane fouling with higher accuracy than PLS.

Keywords: secondary effluent; tertiary treatment; ultrafiltration; artificial neural network; organic matter fractionation

1. Introduction

Wastewater reclamation and reuse is a topic that has been deeply studied in recent years. However, the publication by the European Commission of the proposal for a regulation on minimum requirements for water reuse requires that we urgently revise the efficiency of the processes currently used by the wastewater treatment plants (WWTPs) as tertiary treatments [1]. Particularly, the required validation monitoring implies for the highest quality water (class A) that the implemented processes have to achieve removal efficiencies higher or equal to 5 log of *Escherichia coli* and of the protozoa indicator (*Clostridium perfringens* spores) and higher or equal to 6 log of viruses. This means that the widely used conventional processes, consisting of coagulation–flocculation–sedimentation plus filtration and disinfection with chlorination or UV irradiation, are called into question, as they cannot offer the required efficiencies [2,3]. In addition, it has to be taken into account that bacteria, viruses and protozoa

are biologically and structurally different; therefore the use of one specific chemical or UV irradiation for disinfection may not be efficient for all of them [4–6].

In this context, ultrafiltration (UF) seems to be one of the most suitable techniques to be implemented in the future for reusing wastewater in agriculture, as it achieved a higher removal of pathogens than the above-mentioned processes. This will be especially important in countries such as Spain and other European Mediterranean countries due to the increasing water scarcity.

It has to be highlighted that UF has been used as tertiary treatment for two decades [7,8]. However, the implementation at an industrial scale has not yet been developed. Thus, conventional treatments based on sedimentation and sand filtration followed by disinfection have prevailed in spite of the higher quality of the ultrafiltration permeate [9]. Nevertheless, this scenario may change with the publication of the new legal standards for wastewater reuse, and UF may become one of the most used wastewater reclamation techniques. This means that the main membrane operation problem, i.e., membrane fouling [10], has to be deeply studied.

The main culprit for membrane fouling in UF of secondary effluents is effluent organic matter (EfOM) [11]. EfOM comprises soluble microbial products (SMP), which are compounds from cellular debris or from metabolic reactions of the biomass in the reactor, and the organic matter that flow into the WWTP that have not been degraded by the biomass. This second group of organic matter is divided into the natural organic matter (NOM), which is present in tap water, and the persistent organic compound with anthropogenic origins, such as pharmaceutical compounds and pesticides [12].

It seems obvious that if more information about EfOM in a secondary effluent is available, the membrane fouling will be better predicted during the UF process. For this, two groups of analysis can be found in the literature. On the one hand, SMPs (the main constituent of the EfOM as mentioned above) are measured as the sum of proteins and carbohydrates, which are the main group of substances in the SMPs. SMP production and composition depend on the operational conditions of the biological process and on the raw wastewater itself [13–15]. On the other hand, EfOM has been fractionated by different authors using adsorption resins. Thus, EfOM is divided into the groups of substances separated by each resin. The first fractionations were performed by Leenheer [16] with the aim of characterizing the NOM. Imai et al. [17] divided the EfOM into six fractions (hydrophobic and hydrophilic neutrals, acids and bases). Further works aimed to simplify and adapt this fractionation procedure to obtain information that could correlate the groups of these substances with the membrane fouling potential of the secondary effluent [18,19]. It has to be taken into account that the objective of this work is not to divide the EfOM into the highest number of fractions, nor recover them, but to gain insight on its characteristics in order to predict the membrane fouling.

In this work, model waters were prepared with proteins, carbohydrates and humic acid (main components of SMP) and secondary effluents were taken from a WWTP to perform the following experiments. They were characterized and treated with the adsorption resins, which are used to achieve the organic matter fractionation. Thus, the relationship between SMP substances and organic matter types according to their fractionation with resins was studied. Then, both raw waters (model waters and secondary effluents) and samples from the adsorption processes with the different resins were ultrafiltered. This work is focused on relating the membrane fouling with the UF influent characteristics, so that modeling of experimental results was carried out to predict the ultrafiltered permeate and their flux, from parameters such as chemical oxygen demand (COD), total organic carbon (TOC), protein, and carbohydrate concentrations of the influent. This prediction model will contribute to providing valuable information in order to decide whether ultrafiltration tertiary treatment can be feasible for a particular secondary effluent.

Statistical techniques have been proved to be useful in order to relate one variable to other variables (thus, obtaining a model). The traditional multiple regression model and partial least squares model are two examples of this kind of technique, which can be suitable in order to achieve the aim of this work.

On the other hand, artificial neural networks (ANNs) have been widely used to obtain models that relate some variables (named inputs) to other variables (named outputs), for a lot of different applications (air pollutant concentration [20], energy systems [21], wastewater treatment plant performance [22]), successfully. It is worth noting that each artificial neural network has a particular topology (number of input variables, number of hidden layers, numbers of neurons per layer and number of output variables). As reported by Chaloulakou et al. [20], ANNs achieve equal or higher fitting accuracy than multiple regression models (comparing error indices). However, the physical interpretation of ANNs can be difficult. Modeling of the ultrafiltration membrane fouling from fractionated effluents [18,23,24] and modeling using ANNs [25,26] can be found in the literature. This work is a step forward to the prediction of membrane fouling from the secondary effluent characteristics.

2. Materials and Methods

2.1. Model Waters and the Secondary Effluent

For the model water (MW) synthesis, the following reagents were used: albumin from bovine serum albumin (BSA) as a model protein, xanthan gum (from *Xanthomonas campestris*) as a model carbohydrate and humic acid. All of these chemicals were provided by Sigma-Aldrich (Saint Louis, MO, USA), with the respective references A2153-50G, G1253-500G and 53680. From these chemicals, solutions with only one component (20 mg/L BSA, 10 mg/L xanthan gum and 7 mg/L of humic acid, respectively) and with a mixture of proteins, carbohydrates and humic acids (30 mg/L BSA, 5 mg/L xanthan gum and 7 mg/L of humic acid) were made.

The urban wastewater was taken from the secondary effluent of a WWTP located in Valencia (Spain). Two samples were taken (S1 and S2) over a period of time. S1 was taken in spring (March) and S2 in autumn (September).

Table 1 details the characteristics of model solutions and wastewater samples used in this work. UVA₂₅₄ is the absorbance at 254 nanometers of wave length.

Table 1. Model waters and wastewater nomenclature and compositions.

	Water Type	Nomenclature	COD (mg/L)	TOC (mg/L)	Proteins (mg/L)	Carb. (mg/L)	UVA ₂₅₄
Model water	BSA	MW1	18.0	6.6	21.79	-	-
	Xanthan	MW2	18.8	6.3	-	12.12	-
	Humic acid	MW3	6.0	2.1	-	-	0.18
	BSA + Xanthan + Humic acid	MW4	36.5	13.7	30.51	4.59	0.10
Secondary effluent		S1	30.8	9.3	17.15	6.71	0.20
		S2	17.9	7.6	7.15	4.25	0.12

All the samples were filtered prior to the fractionation step at 0.45 µm using cellulose acetate filters from Hahnemühle. The pH adjustments needed to perform the separation by the resins were carried out by adding hydrochloric acid or sodium hydroxide solutions. Additional data of the S1 and S2 secondary effluents can be observed in Table S1.

2.2. Adsorption onto Resins (Fractionation)

Three commercial resins were used for the removal of different fractions of the EfOM from the wastewater samples and to study the separation of the components of the model solutions. They were Amberlite XAD-4, from SIGMA, Supelite DAX-8 from SUPELCO and Amberlite IRA-958(Cl) from Alfa Aesar, with references XAD4-1KG, 21567-U and 42,702, respectively. Each resin retains certain substances from the natural organic matter by adsorption: strong hydrophobic substances in DAX-8, weak hydrophobic substances in XAD-4 and charged hydrophilic substances in IRA-958. Resins were located in three chromatographic columns with frit and a beaded rim (1000 mL) from

Lenz (Lenz Laborglasinstrumente; Fisher, Germany). DAX-8 and XAD-4 work at an acidic pH, so it is necessary to modify the pH of the sample up to a value of 2 before the contact with these resins. On the contrary, IRA-958 works at a neutral pH, so the pH of the sample has to be adjusted to 7.

All the samples were tested with the three resins separately to evaluate the adsorption capacity of each resin for each substance. Nomenclature used to name the effluents obtained after resin treatment includes the type of water (MWi or Si, according to Table 1 nomenclature) with the resin employed (e.g., MW1-D8 was the effluent collected after the fractionation step of the model water MW1 with DAX-8).

On the other hand, the protocol followed in the present work is that described by Ferrer-Polonio et al. [19]. In this method, the effluent obtained after DAX-8 adsorption was introduced into the XAD-4 column and the effluent of this fractionation step was treated in the IRA-958 column. The final stream was an effluent without strong hydrophobic substances (SHo), weak hydrophobic substances (WHo) and charged hydrophilic substances (CHi). In these tests, the nomenclature used to name the effluent obtained was also the kind of water and the resins used (e.g., MW1-D8 + X4 + IRA).

There is a variety of fractionation protocols available in the literature, which can be used as appropriate. Other authors have followed different protocols in order to obtain different fractions of effluent organic matter, for example Zheng et al. [18] used only XAD-8 and XAD-4 to obtain four fractions, namely, hydrophobic neutrals, colloids, hydrophobic acids, transphilic neutrals and acids and hydrophilics. Additionally, Shon et al. [23] used only XAD-8 and XAD-4 in their study to obtain three different fractions, namely, hydrophobic, transphilic and hydrophilic.

2.3. Ultrafiltration Tests

To perform the ultrafiltration (UF) process, a stirred cell with a capacity of 300 mL was used. This equipment is from Millipore (Bedford, MA, USA) (model XFUF 076 01). In this stirred cell, UF flat sheet membranes of the GR51PP model from Alfa-Laval (Lund, Sweden) were employed. This kind of membrane has an active layer made of polysulfone and a support layer made of polypropylene. Its active area is 40 cm². The molecular weight cut-off is 50 KDa.

Ultrafiltration tests of 30 samples were performed in this work. These samples included the raw model waters and the secondary effluents (without filtration and after filtration at 5 and 0.45 microns) and the different streams obtained after adsorption processes with the resins of all of these effluents.

All the samples, after their characterization according to the methods explained in Section 2.4, were ultrafiltered with the following methodology: (1) 300 mL of sample was introduced into the stirred cell; (2) UF process was performed at 1.5 bar (using compressed air as a transmembrane pressure generator) and at room temperature for at least 2.5 h; (3) permeate flux was measured using a digital scale (Kern, model ABJ) connected to a personal computer via a cable adapter. Permeate was collected, remaining at 4 °C until characterization was performed.

Membrane fouling was modeled using the registered permeate flux decline versus time, fitting it to the classical Hermia's ultrafiltration models adapted to cross-flow filtration, available in the literature [27], in order to infer the fouling mechanism(s).

Additionally, two different models are proposed in this work that could predict (model outputs) the permeate characteristics (ultrafiltration permeate quality) and also the membrane fouling, given as model inputs certain parameters obtained from the wastewater characterization and from the initial influent flux value. The first proposal is a statistical model, which used partial least squares (PLS) method in order to obtain the regression coefficients that correlated the input values to the output values. This work was performed using "Statgraphics Centurion XVI" software from Statpoint Technologies, Inc (The Plains, VA, USA). The second proposal is an artificial neural network model, performed with "MATLAB 2011b" software from MathWorks (Natick, MA, USA). The neural network proposed is a multilayer perceptron (MLP) and uses 15 neurons in the hidden layer. The number of hidden layers and neurons per layer was obtained performing several tests by trial and error in order to obtain the best accuracy with the simplest artificial neural network topology.

The input values for the statistical and artificial neural network models are the COD, TOC, proteins and carbohydrates of the feeds to the UF and the initial permeate water flux (J_0). The output values are the COD, TOC, proteins and carbohydrates of the permeates and also the permeate water flux at the steady-state (J_{ss}).

2.4. Analytical Methods

The model water, secondary effluents, effluents from the resins and permeates of the UF tests were characterized by means of pH, chemical oxygen demand (COD), total organic carbon (TOC), protein and carbohydrate concentrations, UV irradiation at 254 nm of wavelength and conductivity.

pH was measured with a pH meter from Crison (GLP21+ model). For the COD determination COD cell test (4–40 mg/L) and the spectrophotometer model Spectroquant NOVA 30, both from MERCK, were used. TOC was measured with a total organic carbon analyzer from Shimadzu (model TOC-L). Protein and carbohydrate concentrations were measured by the bicinchoninic acid (BCA) method [28] and the anthrone method [29], respectively. UV-254 was achieved with a spectrophotometer DR6000 from Hach Lange (Barcelona, Spain). Conductivity was measured using a CDH-SD1 conductivity meter from Omega Engineering (Manchester, UK).

3. Results

3.1. Treatment of the Secondary Effluent For Its Characterization with Resins

3.1.1. Model Wastewater

The analysis of protein, carbohydrate and humic substances in secondary effluents is of great importance when membrane processes are used as tertiary treatments after a biological process. It is known that the soluble microbial products (SMP) are the main membrane foulants of secondary effluents [30,31]. Their main components are protein, carbohydrate and humic substances [32]. In this way, the effect of the adsorption of these components onto the resins commonly used in the EfOM fractionation of model solutions based on the main SMP components could give relevant information. Results of the removal of these substances by adsorption with the used resins are detailed in Table 2.

Table 2. Removal percentage of COD, proteins, carbohydrates and humic acid (through UVA₂₅₄) from the model waters by adsorption with the used resins.

	COD (%)	Proteins (%)	Carbohydrates (%)	UVA ₂₅₄ (%)
MW1-DAX-8	71.9	97.3	-	-
MW1-XAD-4	2.8	11.4	-	-
MW1-IRA-958	47.8	53.0	-	-
MW2-DAX-8	48.4	-	61.6	-
MW2-XAD-4	25.5	-	29.5	-
MW2-IRA-958	29.8	-	36.8	-
MW3-DAX-8	32.8	-	-	97.3
MW3-XAD-4	43.8	-	-	98.4
MW3-IRA-958	53.1	-	-	97.3
MW4-DAX-8	43.8	59.5	85.4	99.0
MW4-XAD-4	41.1	52.1	52.1	65.4
MW4-IRA-958	58.1	68.9	58.4	78.2

According to the literature [16], compounds of dissolved organic matter (DOM) can be divided into substances with hydrophobic or hydrophilic properties. In this way, humic acids are included in the strong hydrophobic acids, proteins in hydrophilic bases and simple sugars as hydrophilic neutral substances. Taking into account the properties of resins (Section 2.2) used in this work, it can be expected that humic acids should be removed more effectively by DAX-8 and proteins by IRA-958.

Regarding humic acids, they were eliminated from MW3 by the three resins in similar percentages, according to UVA₂₅₄ values, when this substance was the only substrate. However, in comparison with other compounds (in MW4), DAX-8 achieved the highest humic acid removal percentage, as was expected. With regard to proteins (BSA), DAX-8 obtained better results than IRA-958 in MW1. However, in the model water with the three components, IRA-958 was the resin with the highest protein removal, in accordance with the behavior reported in the literature. Finally, carbohydrates should not be preferentially adsorbed by any of the resins, although it can be seen that DAX-8 achieved the highest removal percentages both in MW2 and in MW4.

These results showed that these resins are not specific for eliminating the main components of EfOM. In addition, interactions between proteins, carbohydrates and humic acids conditioned the resins' adsorption behavior.

3.1.2. Secondary Effluents

The parameters of both the secondary effluents differ from each other due to the fact that both samples were taken in different seasons from a WWTP (the water quality depends on multiple factors, such as the intake, the hour of the day, efficiency of the WWTP at any given moment, etc.). In this way, S2 was characterized by lower COD, TOC, protein, carbohydrate and humic substance concentrations than those measured in S1 (Table 3).

Table 3. Characteristics of the different streams in the fractionation experiments of the secondary effluents.

	COD (mg/L)	Proteins (mg/L)	Carbohydrates (mg/L)	UVA ₂₅₄
S1	30.8	17.1	6.7	0.20
S1-DAX-8	19.9	7.4	6.3	0.07
S1-DAX-8 + XAD-4	18.2	3.7	4.5	0.04
S1-DAX-8 + XAD-4 + IRA-958	13.7	1.5	1.2	0.02
S2	17.9	7.1	4.2	0.12
S2-DAX-8	14.7	4.8	3.9	0.06
S2-DAX-8 + XAD-4	11.5	3.4	3.5	0.04
S2-DAX-8 + XAD-4 + IRA-958	9.0	2.6	2.1	0.04
S2-DAX-8 + IRA-958	11.7	3.1	2.1	0.04

Both samples were fractionated following the methodology reported by Ferrer-Polonio et al. [19]. Table 3 shows the stream characterization resulting from the treatment with the three resins of the secondary effluents.

Taking into account the theoretical fractions that each resin adsorbs, Figure 1 shows the organic matter contribution (as percentage of COD) of strong hydrophobic substances (SHo = Si – Si-DAX8), weak hydrophobic substances (WWho = Si-DAX8 – Si-DAX8 + XAD4), charged hydrophilic substances (CHi = Si-DAX8 + XAD4 – Si-DAX8 + XAD4 + IRA958) and neutral hydrophilic substances (NHhi = organic matter of Si-D8 + X4 + IRA) of each secondary effluent.

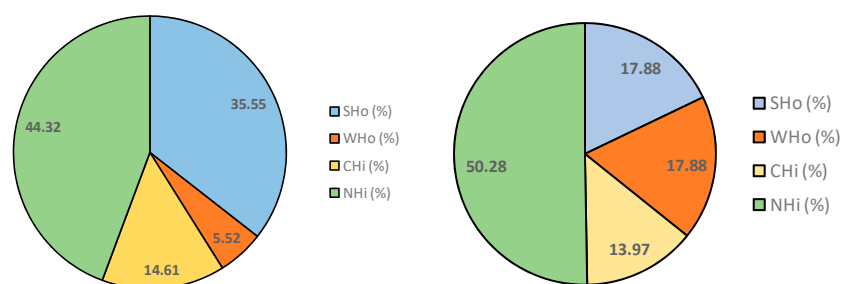


Figure 1. Organic matter type according to the fractionation experiments (S1 on the left and S2 on the right).

It can be seen that neutral and charged hydrophilic substances (CHi + NHi) were similar in both effluents, resulting in 58.9% and 64.3% of the total organic matter of S1 and S2, respectively. These substances are theoretically related to the protein and carbohydrate content (CHi and NHi, respectively).

Regarding that observed in MW, since DAX-8 also retains proteins and carbohydrates, part of these substances were adsorbed before IRA-958 resin treatment. This is explained by the fact that not all protein and carbohydrate types have hydrophilic properties. In this way, humic-bound carbohydrates are hydrophobic acid substances, and some proteins have neutral or basic hydrophobic behavior [33]. Thus, effluent composition influences the preferential adsorption onto one or another resin, which makes the stream characterizations based on DOM fractionation difficult.

Regarding UVA₂₅₄ values (Table 3), which are related to the aromatic compounds such as humic acids [31] and consequently to SHo, it can be seen that the value of this parameter was higher in S1 than in S2. Accordingly, SHo was higher in S1 than in S2.

Additionally, it should be highlighted that hydrophobic substances were lower than hydrophilic ones in both secondary effluents. These results agree with those reported by Tang et al. [30] in their study of fractionation of EfOM from two membrane bioreactors. In this work, concentrations of hydrophilic substances (CHi + NHi) were also higher than the concentration of the hydrophobic ones (SHo + WHo).

In view of achieving a reduction in the duration and cost of the fractionation process, S2 was also fractionated using only two resins, DAX-8 and IRA-958. XAD-4 was not used in this experiment as a consequence of the low removal percentages for the three types of substances analyzed. The results are presented in Table 3. This simplified process eliminated almost the same carbohydrate and humic acid percentages. These results agree with those observed in model waters experiments, in which XAD-4 had the lowest adsorption capacity of proteins and carbohydrates, not only for MW2 and MW3, but also in the multicomponent sample (MW4). Regarding proteins, a simplified process achieved a slightly higher concentration in comparison with the conventional three resin fractionation.

The tests performed with real wastewater suggest that there exist, in the wastewater, other substances that have been not characterized, that are different from the known fractionated substances (named here "others"), and that also affect membrane fouling. This can be inferred from the fact that the three resin in-series fractionation produces a fractionated water that does not contain WHo, SHo, CHi or NHi (due to the affinity of these substances to the used resins: DAX-8, XAD-4 and IRA-958). However, this resulting water fouled the UF membrane. Thus, it is obvious that the original wastewater contained also other compounds not considered in this work.

Additional data regarding the model and secondary effluent wastewater can be found in Table S2.

Habekamp et al. [34] worked with both synthetic and secondary effluent wastewater. These authors used extracellular polymeric substances (EPS) as foulants. They found that the secondary effluent fouled the membrane more than the model EPS wastewater and concluded that proteins and polysaccharides (both SMP) have a big impact on membrane fouling.

3.2. Ultrafiltration

To evaluate the relationship between the different DOM fractions and the membrane fouling, the ultrafiltration experiments of all samples were performed according to the methodology previously explained (Section 2.3).

Figure 2 shows the evolution of normalized flux (J/J_0) over the experimental time. For the raw secondary effluents (Figure 2a), it can be observed that raw S1 had a higher fouling effect on the membrane than in the case of S2, resulting in flux decline percentages of 32.5% and 24.2%, respectively. This behavior was expected due to the higher COD and SMP concentrations in S1.

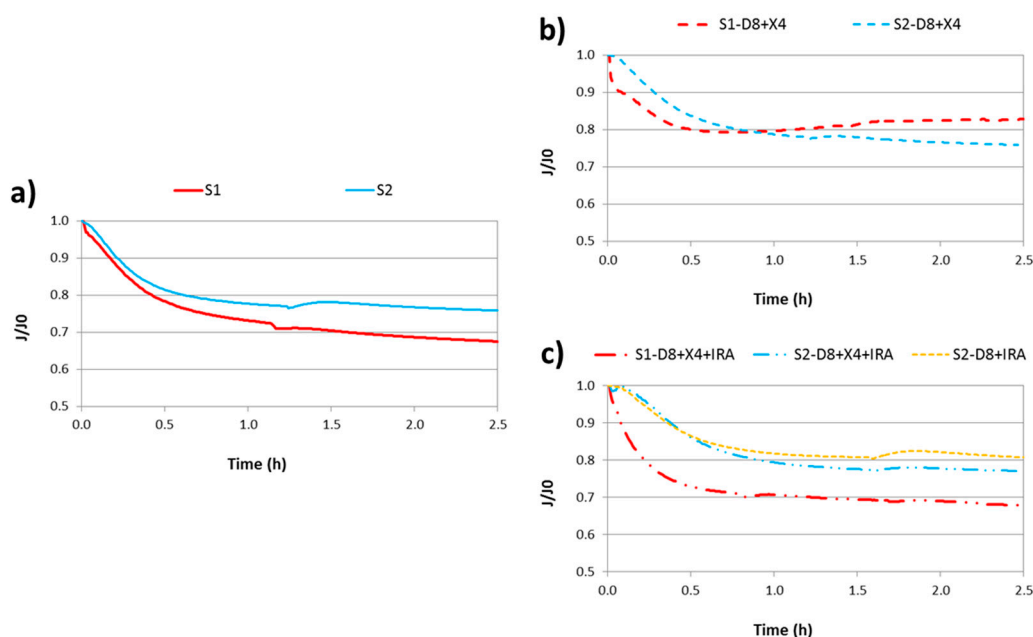


Figure 2. Ultrafiltration tests: (a) raw secondary effluents; (b) effluents after XAD-8 and DAX-4 treatment (hydrophilic substances); (c) effluents after XAD-8, DAX-4 and IRA-598 treatment (neutral hydrophilic substances).

On the other hand, observing Figure 2b, it can be seen that once hydrophobic substances are removed, S1-D8 + X4 showed a higher fouling effect than S2-D8 + X4 in the first hour of experiment. However, from this time, normalized flux of this S1 fraction increased, so at the end of UF test, the flux decline of the S2 fraction was higher than S1. This fact can be related to the fouling mechanism of the secondary effluent S1. According to Hermia's model, cake filtration was the predominant fouling mechanism in S1, while in S2 it was unclear (explained below). Thus, a part or all of the cake formed could be detached from the membrane, resulting in an increased permeate flux.

Finally, observing Figure 2c, it can be seen that the stationary flux of both effluents with only neutral hydrophilic substances (NHi) were similar to their corresponding raw secondary effluents. This means that NHi was the main fouling fraction of the membrane in both samples.

Although results between different figures are not directly comparable since each UF test was performed with a pristine membrane and water permeability was not the same (this is the reason why fluxes are normalized dividing by J_0), it seems clear that NHi was the main fouling fraction. In fact, NHi is the most predominant EfOM fraction of S1 and S2, as commented above. This implied that carbohydrates played the most important role in membrane fouling, which is in accordance with that reported by other researchers [15,35].

Furthermore, considering that the membrane has a contact angle of about 54.6° [36] and thus it is of hydrophilic kind, it seems clear that it has more affinity for hydrophilic substances (like NHi and CHi) that can foul the membrane to a larger extent.

Regarding the UF stream obtained from the simplified fractionation method, it can be concluded that a similar final DOM fraction was achieved with two and three resins, as flux decline profiles were very similar.

Hermia's fouling mechanisms were applied in order to infer the predominant fouling mechanism in the ultrafiltration of model waters and wastewaters (and their respective fractions). Thus, the experimental data (flux decline versus time) have been fitted to three of the four Hermia's model equations that describe the fouling mechanisms to complete blocking, intermediate blocking, and cake filtration, in order to evaluate the best fitting. The standard pore blocking model did not fit the experimental data at all, perhaps due to the size of the natural organic matter than can be equal to or higher than the pore size of the membrane (50 KDa cut-off). This is the case for BSA (65KDa, [37])

and xanthan (1100–8700 KDa, [38]), but not humic acid (227.17 Da, [39]). It is worth noting that the standard pore blocking model is for a dead-end, and it has never been adapted to cross-flow. This may also be the reason for the low fitting accuracy obtained in that case.

Table S3 shows the accuracy of Hermia's ultrafiltration fouling models in terms of the coefficient of determination (R-squared, R^2) and population standard deviation (SD_p). In this table, values in bold mean that the corresponding Hermia's model fits the best.

The secondary effluent S1 has cake filtration as a predominant Hermia's fouling mechanism (this could imply that a gel layer is formed on the membrane surface, and solutes can be deposited on the membrane and also on the gel layer in terms of Hermia's theory), while in the case of the secondary effluent S2, the predominant Hermia's fouling mechanism is unclear. For S2, both complete and intermediate blocking had similar R^2 . That is, the fitting accuracy of both blocking mechanisms is high and its R-squared values are very similar. The former is not the expected fouling mechanism, and the reason could be that the difference in the R-square value of the fitting to intermediate fouling and complete blocking is negligible. Then, complete blocking should be, supposedly, the predominant Hermia's fouling mechanism. Another argument to reinforce this assumption is that S1 has a higher concentration of proteins than S2, and proteins are bigger in size than the Molecular Weight Cut-Off (MWCO) of the membrane and could promote the formation of a cake layer in the membrane used in the ultrafiltration of S1.

It is worth noting that the predominant Hermia's fouling mechanism of ultrafiltration tests performed with different feed compositions may differ from one test to another.

Corbatón et al. [40] evaluated the fitting accuracy of the models to the experimental data, comparing the R^2 and standard deviation (SD) values among the tests performed, as the authors of this work did. They also concluded that a combined model (complete blocking and cake filtration) fitted the best when they used BSA as a foulant. They found, also, that a standard blocking fouling model did not fit well to the experimental data, and they consider that this could be due to the fact that the size of the BSA is higher than the pore size of the membrane.

Maruyama et al. [41] identified protein fouling as a problem for ultrafiltration. They conducted experiments with BSA, as the authors of the present work did. The test performed in this work with model water MW1 (20 g/L BSA) showed a clear flux decline over time, confirming Maruyama's statement.

Focusing on the simulated secondary effluents, Soler-Cabezas et al. [42], found that the predominant Hermia's fouling mechanism was intermediate blocking (instead of complete blocking in the case of the present work) when they worked with the simulated secondary treatment effluent wastewater consisting of BSA and dextran. However, the results cannot be directly compared to ours, as they used a membrane of 200 KDa of MWCO and dextran. It is worth noting that the dextran molecule is 200 KDa in size, very similar to the MWCO of the membrane, which means that Hermia's theory predicts that the predominant fouling mechanism could be intermediate blocking (if we consider very similar sizes) or the cake layer (if we consider the fact that the solute size is larger than the pore size). Finally, intermediate blocking was reported by these authors to be the predominant model.

With other substances or effluents, many other results about flux modelling in UF processes can be found. For example, Vincent et al. [43] ultrafiltered polyethylene glycol using ceramic membranes, and they found that the predominant fouling mechanism was the cake layer, followed by intermediate blocking using Hermia's models.

Mah et al. [44] found that cake filtration was the predominant Hermia's fouling mechanism when conducting ultrafiltration of palm oil, oleic acid and glycerin. They developed a multistage Hermia's fouling model that considered different fouling mechanisms depending on the time considered (e.g., a different model at the beginning and the end of the test).

Figure 3 shows the fitting of the experimental values to each Hermia's model for tests S1 and S2.

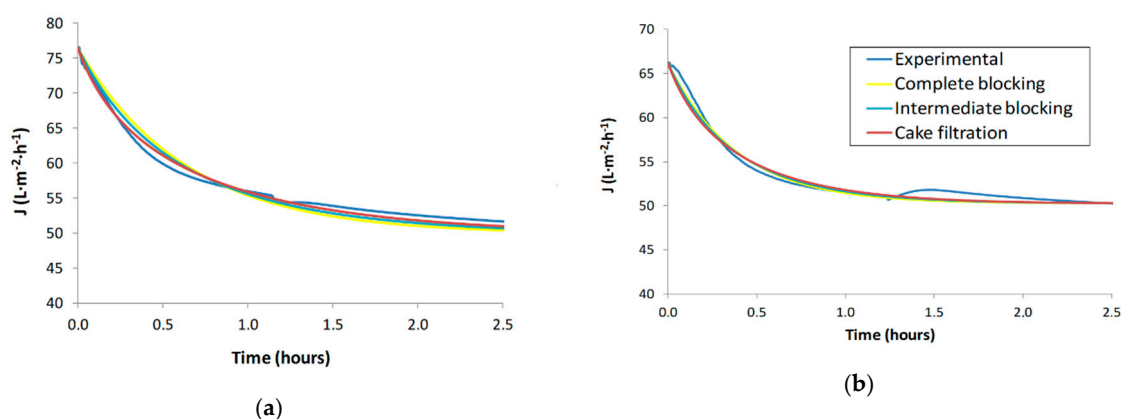


Figure 3. Fitting of Hermia's model of secondary effluent wastewaters: (a) S1 (5-micron filtered), (b) S2 (5-micron filtered).

As can be seen in Figure 3, Hermia's model predictions are quite similar among the two tests. In the case of S2, the fitting is more difficult than in the case of S1 due to the significant flux decline trend in S2 that has anomalies (convex curvature at the beginning of the test instead of concave curvature and a flux upturn at about 1.5 h). Haberkamp et al. [34] encountered a similar trend in shape upturn of permeate flux during the ultrafiltration of macromolecular dissolved organic compounds. It is worth noting that the trend of the theoretical values (Hermia's models) in S2 tends to correct the aforementioned anomalies.

Saha et al. [45] ultrafiltered humic acids solutions in a dead-end cell using a flat-sheet membrane of polyethersulfone of 50 KDa (a similar membrane to that of the authors of this work). They used also the Hermia's models to fit the experimental data to the fouling model. However, they used the linearized equations of Hermia, obtaining R^2 values higher than 90% in all cases. Their COD rejection of humic acid (as model water) value was 85.44%, which, as expected, is higher than the rejection found in this work (60.93%) due to the higher transmembrane pressure in the case of Saha et al. (2.07 vs. 1.5 bar).

Acero et al. [46] also worked with municipal secondary effluents. They ultrafiltered their secondary effluent with a 20 KDa polyethersulphone ultrafiltration membrane at 4 bar of transmembrane pressure. They calculated the rejection of COD, TOC, UVA₂₅₄ and turbidity. Their rejections were higher than that obtained by the authors of the present work, as expected when taking into account the fact that the molecular cut-off of their membrane is lower than that used in this work (20 vs. 50 KDa), and also due to the fact that the pressure in their work is also higher (4 vs. 1.5 bar).

Muthukumar et al. [47] also evaluated the performance of ultrafiltration membranes applied to a secondary effluent. However, they used two different kinds of membranes than those used in this work, namely, spiral UF (1 KDa) and ceramic tubular UF (25 KDa). They used the rejection coefficients of COD, UV₂₅₄, color and turbidity as performance indicators. They found a higher rejection than the authors of this work, maybe due to the fact that the MWCO is higher (50 KDa) in our case. On the other hand, the flux decline evolution of the spiral UF membrane is quite similar to that obtained in this work. However, the flux decline in the case of the tubular UF membrane is very different (it remains almost constant).

3.3. Predictive Models: Permeate Water Quality and Fouling Prediction Modeling

3.3.1. Multiple Regression and Partial Least Squares Statistical Model

The multiple regression technique, available in Statgraphics Centurion, uses ordinary least squares to relate one parameter (dependent variable) to multiple parameters (independent variables).

Conductivity was not included in the regression since its contribution to the model was not significant.

The relationships (equations) obtained are shown in Table 4.

Table 4. Equations from the multiple regression statistical model (correlation coefficients) for the sample after ultrafiltration tests (permeate).

$\text{COD}_p = -2.83664 + 0.188945 \cdot \text{COD}_f + 2.20282 \cdot \text{TOC}_f - 0.465345 \cdot \text{Proteins}_f - 0.43744 \cdot \text{Carbohydrates}_f + 0.0306219 \cdot J_0$
$\text{TOC}_p = -0.73319 + 0.065278 \cdot \text{COD}_f + 0.749591 \cdot \text{TOC}_f - 0.149942 \cdot \text{Proteins}_f - 0.115399 \cdot \text{Carbohydrates}_f + 0.00795281 \cdot J_0$
$\text{Proteins}_p = -0.63856 + 0.0850229 \cdot \text{COD}_f + 0.513374 \cdot \text{TOC}_f - 0.0335743 \cdot \text{Proteins}_f + 0.177371 \cdot \text{Carbohydrates}_f - 0.0159037 \cdot J_0$
$\text{Carbohydrates}_p = 0.0000457033 + 0.0480191 \cdot \text{COD}_f + 0.389582 \cdot \text{TOC}_f - 0.0521522 \cdot \text{Proteins}_f + 0.146084 \cdot \text{Carbohydrates}_f - 0.0103836 \cdot J_0$
$J_{ss} = 37.4286 + 0.657559 \cdot \text{COD}_f - 1.83176 \cdot \text{TOC}_f - 0.220289 \cdot \text{Proteins}_f - 1.27337 \cdot \text{Carbohydrates}_f + 0.305038 \cdot J_0$

where COD, TOC, Proteins and carbohydrates are denoted in terms of mg/L and J_0 and J_{ss} are in terms of $\text{L} \cdot \text{m}^{-2} \cdot \text{h}^{-1}$. Subscript “p” indicates that this parameter corresponds to the ultrafiltrated permeate stream. Parameters with “f” subscript correspond to the influent.

It should be highlighted that Hermia’s constant was not included in this model because the correlation between inputs and outputs indicated no statistical significance (p -values were higher than 0.05) for this parameter.

The partial least squares (PLS) technique, also available in Statgraphics Centurion, leads to correlation coefficients that correlate inputs (COD_f , TOC_f , proteins_f and carbohydrates_f of the influent and initial water flux J_0) and outputs (COD_p , TOC_p , proteins_p , carbohydrates_p of permeate, and steady-state water flux J_{ss}).

The correlation coefficients matrix obtained by the analysis of PLS leads, in this case, to the same equations previously obtained in Table 4. However, PLS provides, in addition, an ANOVA statistical analysis that showed that the correlation between inputs and outputs was significant, as its p -values were lower than 0.05 (5%) (see Table 5).

Table 5. ANOVA analysis.

Model Parameter	p -Value
UF_COD	0.0006786
UF_TOC	0.0017354
UF_PROTEINS	0.0351548
UF_CARBOHYDRATES	0.0189849
J_{ss}	0.0001584

3.3.2. Artificial Neural Network Model

Figure 4 shows the fitting accuracy (in terms of R , not R^2) of the trained ANN during the training, validation and test steps (66.66% samples for training, 16.66% for validation and 16.66% for testing). These percentages are very close to the recommended 80% for the training step and 20% for the test step if we consider the training group as the sum of 66.66% and 16.16%, that is to say, 83.33%. R -squared values ranges from 0 to 1 (or from 0% to 100%, equivalently) and their meaning is the fitting accuracy of the model to the experimental data, explained as follows: 0% means no fitting at all and 100% means a perfect fitting.

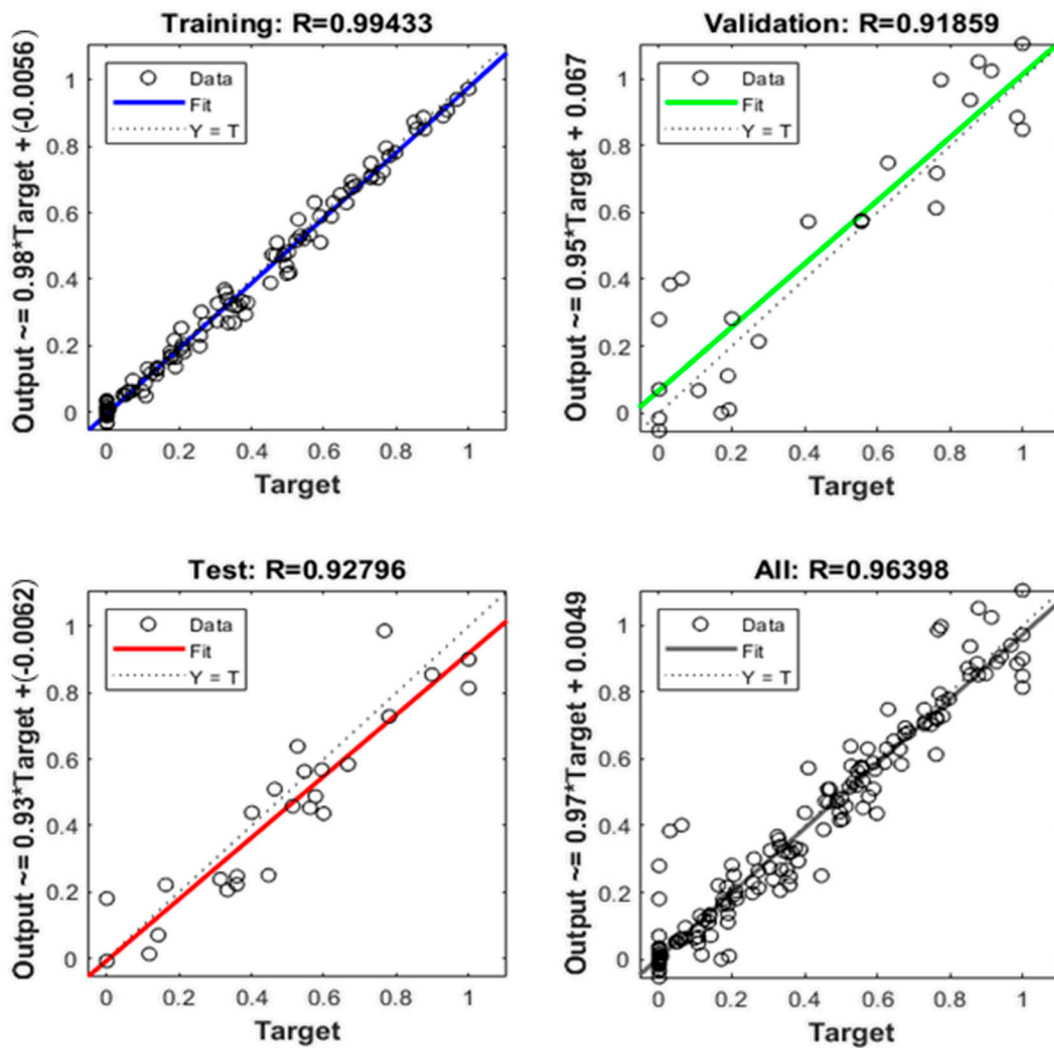


Figure 4. Neural network fitting accuracy (R).

As can be seen in Figure 4, the global R^2 of the model obtained is 0.9292, that is to say, 92.92%. In addition, the bisecting line of the four scatter plots (training, validation, test and all) is homogeneously covered with dots, and the line of their respective regressions is closer to the bisecting line. Then, it can be concluded that this model has good fitting accuracy.

3.3.3. Models Comparison

To compare the prediction accuracy of the two models developed, both raw effluents were tested when given the data shown in Table 6 as input values.

Table 6. Input values of known samples (at 1.5 bar pressure and the Alfa-Laval GR51PP membrane).

Sample	COD (mg/L)	TOC (mg/L)	Proteins (mg/L)	Carbohydrates (mg/L)	J_0 (L/m ² ·h)
S1 (5 micron)	25.75	16.73	7.03	9.18	76.50
S2 (5 micron)	19.80	7.55	3.98	7.68	66.24

A prediction of the ultrafiltered water quality and membrane fouling that would be achieved for these cases is shown in Table 7. The data selected belong to the S1 and S2 (5 micron filtered) tests, the most difficult tests to predict, as they are real secondary effluents, not model solutions.

Table 7. Experimental values and predicted for both models (partial least squares (PLS) and artificial neural network (ANN)).

Sample	Model	COD _p (mg/L)	TOC _p (mg/L)	Proteins _p (mg/L)	Carbohydrates _p (mg/L)	J ₀ (L/m ² ·h)
S1 (5 micron)	Real	19.0	6.7	10.7	6.8	49.9
	PLS	13.7	5.1	5.7	4.2	48.2
	ANN	20.8	7.8	12.8	8.7	51.7
S2 (5 micron)	Real	17.7	7.2	5.9	4.4	50.2
	PLS	14.6	5.3	4.4	3.4	49.9
	ANN	17.3	6.9	5.7	3.6	47.9

In Table 8, the deviation of the predicted values from the experimental values is shown (as percentages).

Table 8. The deviation of predicted values from experimental values for both models (PLS and ANN).

Sample	Model	COD _p (%)	TOC _p (%)	Proteins _p (%)	Carbohydrates _p (%)	J ₀ (%)
S1 (5 micron)	PLS	27.76	26.87	46.33	38.37	3.28
	ANN	9.53	12.11	19.72	28.64	6.14
S2 (5 micron)	PLS	17.53	27.06	26.15	20.85	0.72
	ANN	2.03	3.53	3.47	16.53	4.62

As can be seen in Table 8, the ANN model predicted the experimental values more accurately (taking into account the variation percentage) than the PLS model, with the exception of the steady-state flux J_{ss} . In addition, it is known that ANNs can achieve better results than multiple (linear) regression, as the former can include possible non-linear effects [48]. It is worth noting that the S2 test fitted better than S1 to both statistical and ANN models, probably due to unexpected results of S1-D8 + X4.

Other authors such as Delgrange-Vincent et al. [26] also worked with ANNs. These authors focused on the “long term prediction” of fouling. They evaluated the water quality in terms of dissolved oxygen, temperature and redox potential since their aim was to obtain drinking water by ultrafiltration.

4. Conclusions

In the tests performed with model wastewaters fractionation, humic acids were eliminated in MW3 (only humic acids in its composition) by the three resins in similar percentages. However, in MW4 (three substances in the composition), DAX-8 resin achieved the higher humic acid removal percentage. In terms of proteins, in MW1 (only BSA protein), proteins were removed by DAX-8 resin at a higher percentage. However, in MW4 (three substances), IRA-958 resin removed proteins at a higher percentage. Regarding carbohydrates, they should not be preferentially adsorbed by any of the resins; however, DAX-8 resin had the highest removal percentages in MW2 (only xanthan) and MW4. It seems clear that interactions between proteins, carbohydrates and humic acids condition the resins' adsorption behavior.

In regard to the secondary effluent fractionation tests, DAX-8 resin removed humic acids and proteins at a higher percentage. IRA-958 resin had the highest carbohydrate removal percentage. Turning to another issue, hydrophilic substance (CHi + NHi) concentration was higher than

hydrophobic (SHo + WHo) substance concentration. The secondary effluent wastewaters analyzed had a high concentration of hydrophilic neutral substances (and “others”), followed by strong hydrophobic substances.

The authors proposed a modified Ferrer-Polonio et al. [19] resin fractionation protocol, in which only two resins in series (DAX-8 and IRA-958) are used, instead of DAX-8, XAD-4 and IRA-958 resins in series. This modified protocol results in cost and fractionation time reduction, and provides very similar results in terms of COD, protein and carbohydrate concentrations.

Regarding the ultrafiltration of the secondary effluent wastewater, neutral hydrophilic substances (NH_i) fouled the most, probably due to carbohydrates. There is a relationship between groups of substances with respect to hydrophilicity/hydrophobicity and SMP (proteins, carbohydrates and humic acids). Similar DOM fractions were obtained with three and two resins, as the flux decline profile was very close.

The secondary effluent fouling mechanism was found to be the cake filtration in the S1 sample and complete blocking in the S2 sample. In order to model membrane fouling, it is useful to study SMP rather than the nature of the substances obtained by fractionation.

Two different models (partial least squares and artificial neural network, respectively) have been developed. Both models can predict the ultrafiltration permeate flux at steady state (related to the fouling) and permeate quality. The PLS statistic model predicts the ultrafiltration permeate of water and fouling worse than the neural network model, which provided more accurate predictions. The input data the models need are the secondary effluent wastewater characterization in terms of COD, TOC, proteins and carbohydrates and the initial water flux.

Supplementary Materials: The following are available online at <http://www.mdpi.com/2073-4441/12/7/1975/s1>, Table S1: Wastewater characterization of S1 and S2. Table S2: TOC of model wastewaters. Table S3: Fitting accuracy of experimental flux decline to Hermia’s ultrafiltration models.

Author Contributions: Conceptualization, J.A.M.-R., M.C.V.-V.; methodology, J.A.M.-R., E.F.-P.; software, A.A.B.-Z.; validation, J.A.M.-R., J.L.S.-C.; formal analysis, A.A.B.-Z., J.L.S.-C.; investigation, A.A.B.-Z., J.L.S.-C.; resources, J.A.M.-R.; data curation, A.A.B.-Z., J.L.S.-C.; writing—original draft preparation, J.L.S.-C.; writing—review and editing, J.L.S.-C., E.F.-P., J.A.M.-R., M.C.V.-V.; visualization, A.A.B.-Z.; supervision, J.A.M.-R., M.C.V.-V.; project administration, J.A.M.-R.; funding acquisition J.A.M.-R. All authors have read and agreed to the published version of the manuscript.

Funding: This study was funded by Generalitat Valenciana (Project AICO 18/319).

Acknowledgments: Authors are very thankful for the support from Generalitat Valenciana (Spain).

Conflicts of Interest: The authors declare no conflict of interest.

Abbreviations

WWTP	wastewater treatment plant
UV	ultraviolet radiation
EfOM	effluent organic matter
NOM	natural organic matter
SMP	soluble microbial products
EPS	extracellular polymeric substances
SHo	strong hydrophobic substances
WHo	weak hydrophobic substances
Chi	charged hydrophilic substances
NHi	neutral hydrophilic substances
COD	chemical oxygen demand
TOC	total organic carbon
UVA ₂₅₄	absorbance at 254 nm wavelength
PLS	partial least squares
ANN	artificial neural network

References

1. European Commission—Environment. Available online: <https://ec.europa.eu/environment/water/reuse.htm> (accessed on 28 December 2019).
2. Rippey, S.R.; Watkins, W.D. Comparative rates of disinfection of microbial indicator organisms in chlorinated sewage effluents. *Water Sci. Technol.* **1992**, *26*, 2185–2189. [[CrossRef](#)]
3. Mounaouer, B.; Abdennaceur, H. Modeling and kinetic characterization of wastewater disinfection using chlorine and UV irradiation. *Environ. Sci. Pollut. Res.* **2016**, *23*, 19861–19875. [[CrossRef](#)]
4. Hijnen, W.A.M.; Beerendonk, E.F.; Medema, G.J. Inactivation credit of UV radiation for viruses, bacteria and protozoan (oo)cysts in water: A review. *Water Res.* **2006**, *40*, 3–22. [[CrossRef](#)] [[PubMed](#)]
5. Cervero-Aragó, S.; Rodríguez-Martínez, S.; Puertas-Bennasar, A.; Araujo, R.M. Effect of common drinking water disinfectants, chlorine and heat, on free Legionella and amoebae-associated Legionella. *PLoS ONE* **2015**, *10*, 1–18. [[CrossRef](#)] [[PubMed](#)]
6. Anfruns-Estrada, E.; Bruguera-Casamada, C.; Salvadó, H.; Brillas, E.; Sirés, I.; Araujo, R.M. Inactivation of microbiota from urban wastewater by single and sequential electrocoagulation and electro-Fenton treatments. *Water Res.* **2017**, *126*, 450–459. [[CrossRef](#)] [[PubMed](#)]
7. Tchobanoglous, G.; Darby, J.; Bourgeois, K.; McArdle, J.; Genest, P.; Tylla, M. Ultrafiltration as an advanced tertiary treatment process for municipal wastewater. *Desalination* **1998**, *119*, 315–321. [[CrossRef](#)]
8. Lubello, C.; Gori, R.; De Bernardinis, A.M.; Simonelli, G. Ultrafiltration as tertiary treatment for industrial reuse. *Water Sci. Technol. Water Supply* **2003**, *3*, 161–168. [[CrossRef](#)]
9. Illueca-Muñoz, J.; Mendoza-Roca, J.A.; Iborra-Clar, A.; Bes-Piá, A.; Fajardo-Montañana, V.; Martínez-Francisco, F.J.; Bernacer-Bonora, I. Study of different alternatives of tertiary treatments for wastewater reclamation to optimize the water quality for irrigation reuse. *Desalination* **2008**, *222*, 222–229. [[CrossRef](#)]
10. Delgado, S.; Díaz, F.; Vera, L.; Díaz, R.; Elmaleh, S. Modelling hollow-fibre ultrafiltration of biologically treated wastewater with and without gas sparging. *J. Memb. Sci.* **2004**, *228*, 55–63. [[CrossRef](#)]
11. Filloux, E.; Labanowski, J.; Croue, J.P. Understanding the fouling of UF/MF hollow fibres of biologically treated wastewaters using advanced EfOM characterization and statistical tools. *Bioresour. Technol.* **2012**, *118*, 460–468. [[CrossRef](#)]
12. Shon, H.K.; Vigneswaran, S.; Snyder, S.A. Effluent Organic Matter (EfOM) in Wastewater: Constituents, Effects, and Treatment. *Crit. Rev. Environ. Sci. Technol.* **2007**, *36*, 327–374. [[CrossRef](#)]
13. Wang, Z.P.; Zhang, T. Characterization of soluble microbial products (SMP) under stressful conditions. *Water Res.* **2010**, *44*, 5499–5509. [[CrossRef](#)] [[PubMed](#)]
14. Ferrer-Polonio, E.; White, K.; Mendoza-Roca, J.A.; Bes-Piá, A. The role of the operating parameters of SBR systems on the SMP production and on membrane fouling reduction. *J. Environ. Manag.* **2018**, *228*, 205–212. [[CrossRef](#)]
15. Ferrer-Polonio, E.; Fernández-Navarro, J.; Alonso-Molina, J.L.; Bes-Piá, A.; Mendoza-Roca, J.A. Influence of organic matter type in wastewater on soluble microbial products production and on further ultrafiltration. *J. Chem. Technol. Biotechnol.* **2018**, *93*, 3284–3291. [[CrossRef](#)]
16. Leenheer, J.A. Comprehensive Approach to Preparative Isolation and Fractionation of Dissolved Organic Carbon from Natural Waters and Wastewaters. *Environ. Sci. Technol.* **1981**, *15*, 578–587. [[CrossRef](#)] [[PubMed](#)]
17. Imai, A.; Fukushima, T.; Matsushige, K.; Kim, Y. Characterization of dissolved organic matter in effluents from wastewater treatment plants. *Water Res.* **2002**, *36*, 859–870. [[CrossRef](#)]
18. Zheng, X.; Khan, M.T.; Croué, J.P. Contribution of effluent organic matter (EfOM) to ultrafiltration (UF) membrane fouling: Isolation, characterization, and fouling effect of EfOM fractions. *Water Res.* **2014**, *65*, 414–424. [[CrossRef](#)]
19. Ferrer-Polonio, E.; McCabe, M.; Mendoza-Roca, J.A.; Vincent-Vela, M.C. Fractionation of secondary effluents of wastewater treatment plants in view of the evaluation of membrane fouling in a further ultrafiltration step. *J. Chem. Technol. Biotechnol.* **2018**, *93*, 1495–1501. [[CrossRef](#)]
20. Chaloulakou, A.; Grivas, G.; Spyrellis, N. Neural network and multiple regression models for PM10 prediction in Athens: A comparative assessment. *J. Air Waste Manag. Assoc.* **2003**, *53*, 1183–1190. [[CrossRef](#)]
21. Kalogirou, S.A. Applications of artificial neural-networks for energy systems. *Appl. Energy* **2000**, *67*, 17–35. [[CrossRef](#)]

22. Hamed, M.M.; Khalafallah, M.G.; Hassanien, E.A. Prediction of wastewater treatment plant performance using artificial neural networks. *Environ. Model. Softw.* **2004**, *19*, 919–928. [[CrossRef](#)]
23. Shon, H.K.; Vigneswaran, S.; Kim, I.S.; Cho, J.; Ngo, H.H. Fouling of ultrafiltration membrane by effluent organic matter: A detailed characterization using different organic fractions in wastewater. *J. Memb. Sci.* **2006**, *278*, 232–238. [[CrossRef](#)]
24. Marhaba, T.F. Fluorescence technique for rapid identification of DOM fractions. *J. Environ. Eng.* **2000**, *126*. [[CrossRef](#)]
25. Teodosiu, C.; Pastravanu, O.; Macoveanu, M. Neural network models for ultrafiltration and backwashing. *Water Res.* **2000**, *34*, 4371–4380. [[CrossRef](#)]
26. Delgrange-Vincent, N.; Cabassud, C.; Cabassud, M.; Durand-Bourlier, L.; Laîné, J.M. Neural networks for long term prediction of fouling and backwash efficiency in ultrafiltration for drinking water production. *Desalination* **2000**, *131*, 353–362. [[CrossRef](#)]
27. Vincent Vela, M.C.; Álvarez Blanco, S.; Lora García, J.; Bergantiños Rodríguez, E. Analysis of membrane pore blocking models adapted to crossflow ultrafiltration in the ultrafiltration of PEG. *Chem. Eng. J.* **2009**, *149*, 232–241. [[CrossRef](#)]
28. Zuriaga-Agustí, E.; Bes-Piá, A.; Mendoza-Roca, J.A.; Alonso-Molina, J.L. Influence of extraction methods on proteins and carbohydrates analysis from MBR activated sludge flocs in view of improving EPS determination. *Sep. Purif. Technol.* **2013**, *112*, 1–10. [[CrossRef](#)]
29. Frolund, B.; Palmgren, R.; Keiding, K.; Nielsen, P.H. Extraction of extracellular polymers from activated sludge using a cation exchange resin. *Water Res.* **1996**, *30*, 1749–1758. [[CrossRef](#)]
30. Juang, L.C.; Tseng, D.H.; Chen, Y.M.; Semblante, G.U.; You, S.J. The effect soluble microbial products (SMP) on the quality and fouling potential of MBR effluent. *Desalination* **2013**, *326*, 96–102. [[CrossRef](#)]
31. Ayache, C.; Pidou, M.; Croué, J.P.; Labanowski, J.; Poussade, Y.; Tazi-Pain, A.; Keller, J.; Gernjak, W. Impact of effluent organic matter on low-pressure membrane fouling in tertiary treatment. *Water Res.* **2013**, *47*, 2633–2642. [[CrossRef](#)]
32. Barker, D.J.; Stuckey, D.C. A review of soluble microbial products (SMP) in wastewater treatment systems. *Water Res.* **1999**, *33*, 3063–3082. [[CrossRef](#)]
33. Tipping, E. *Cation Binding by Humic Substances*; Cambridge University Press: Cambridge, UK, 2002.
34. Haberkamp, J.; Ernst, M.; Böckelmann, U.; Szewzyk, U.; Jekel, M. Complexity of ultrafiltration membrane fouling caused by macromolecular dissolved organic compounds in secondary effluents. *Water Res.* **2008**, *42*, 3153–3161. [[CrossRef](#)]
35. Yigit, N.O.; Harman, I.; Civelekoglu, G.; Koseoglu, H.; Cicek, N.; Kitis, M. Membrane fouling in a pilot-scale submerged membrane bioreactor operated under various conditions. *Desalination* **2008**, *231*, 124–132. [[CrossRef](#)]
36. Yammine, S.; Rabagliato, R.; Vitrac, X.; Peuchot, M.M.; Ghidossi, R. Selecting ultrafiltration membranes for fractionation of high added value compounds from grape pomace extracts. *OENO One* **2019**, *53*, 487–497. [[CrossRef](#)]
37. Babcock, J.J.; Brancaleon, L. Bovine serum albumin oligomers in the E- and B-forms at low protein concentration and ionic strength. *Int. J. Biol. Macromol.* **2014**, *53*, 42–53. [[CrossRef](#)]
38. Zirnsak, M.A.; Boger, D.V. Axisymmetric entry flow of semi-dilute xanthan gum solutions: Prediction and experiment. *J. Non Newton. Fluid Mech.* **1998**, *79*, 105–136. [[CrossRef](#)]
39. PubChem. Humic Acid. Available online: <https://pubchem.ncbi.nlm.nih.gov/compound/Humic-acid> (accessed on 1 March 2020).
40. Corbatón-Báguena, M.J.; Álvarez-Blanco, S.; Vincent-Vela, M.C. Fouling mechanisms of ultrafiltration membranes fouled with whey model solutions. *Desalination* **2015**, *360*, 87–96. [[CrossRef](#)]
41. Maruyama, T.; Katoh, S.; Nakajima, M.; Nabetani, H. Mechanism of bovine serum albumin aggregation during ultrafiltration. *Biotechnol. Bioeng.* **2001**, *75*, 233–238. [[CrossRef](#)]
42. Soler-Cabezas, J.L.; Torà-Grau, M.; Vincent-Vela, M.C.; Mendoza-Roca, J.A.; Martínez-Francisco, F.J. Ultrafiltration of municipal wastewater: Study on fouling models and fouling mechanisms. *Desalin. Water Treat.* **2015**, *56*, 3427–3437. [[CrossRef](#)]
43. Vela, M.C.V.; Blanco, S.Á.; García, J.L.; Rodríguez, E.B. Analysis of membrane pore blocking models applied to the ultrafiltration of PEG. *Sep. Purif. Technol.* **2008**, *62*, 489–498. [[CrossRef](#)]

44. Mah, S.K.; Chuah, C.K.; Cathie Lee, W.P.; Chai, S.P. Ultrafiltration of palm oil-oleic acid-glycerin solutions: Fouling mechanism identification, fouling mechanism analysis and membrane characterizations. *Sep. Purif. Technol.* **2012**, *98*, 419–431. [[CrossRef](#)]
45. Saha, S.; Das, C. Analysis of Fouling Characteristics and Flux Decline during Humic Acids Batch Ultrafiltration. *J. Chem. Eng. Process Technol.* **2015**, *6*. [[CrossRef](#)]
46. Acero, J.L.; Benitez, F.J.; Leal, A.I.; Real, F.J.; Teva, F. Membrane filtration technologies applied to municipal secondary effluents for potential reuse. *J. Hazard. Mater.* **2010**, *177*, 390–398. [[CrossRef](#)] [[PubMed](#)]
47. Muthukumar, S.; Nguyen, D.A.; Baskaran, K. Performance evaluation of different ultrafiltration membranes for the reclamation and reuse of secondary effluent. *Desalination* **2011**, *279*, 383–389. [[CrossRef](#)]
48. Pao, H.T. A comparison of neural network and multiple regression analysis in modeling capital structure. *Expert Syst. Appl.* **2008**, *35*, 720–727. [[CrossRef](#)]



© 2020 by the authors. Licensee MDPI, Basel, Switzerland. This article is an open access article distributed under the terms and conditions of the Creative Commons Attribution (CC BY) license (<http://creativecommons.org/licenses/by/4.0/>).